



# OPTIMIZATION OF COWL AND RAMP ANGLES OF HYPERSONIC INTAKE OF SCRAMJET ENGINE

Nayem Shaik<sup>1</sup>, Sreenivasa Rao M<sup>2</sup>, Rambabu Palli<sup>3a</sup>, Sanyasi Naidu Gogada<sup>3b</sup>, Harsha Vardhan Silugapu<sup>3c</sup>, Naveen Redrothu<sup>3d</sup>.

<sup>1</sup>Assistant Professor in Mechanical Engineering, Godavari Institute of Engineering & Technology(A), Andhra Pradesh, India,

<sup>2</sup>Professor in Mechanical Engineering, Godavari Institute of Engineering & Technology(A), Andhra Pradesh, India,

<sup>3a,3b,3c,3d</sup>B.Tech Student in Mechanical Engineering, Godavari Institute of Engineering & Technology(A), Andhra Pradesh, India,

**Abstract:** Air breathing engines are widely used in aircraft and missile applications. These air breathing engines will work efficiently in supersonic and hypersonic conditions only. Supersonic air breathing engines work in the range of Mach 3 to 5 and hypersonic air breathing engines work on above Mach 5 or 6. The hypersonic air breathing engines are known as scramjet engines. Air breathing engines efficiency was increased by increasing the pressure recovery or pressure at the outlet of the inlet. Thus with the increasing efficiency of hypersonic inlet diffusers, it directly improves the efficiency of the hypersonic air breathing engine. In this paper numerical analysis was conducted to improve the efficiency of hypersonic inlet diffusers by varying cowl and ramp geometry (angle and lengths). It is observed that with the increase of lengths of ramp outlet Mach number and pressure are increased.

**Keywords:** Hypersonic air breathing engine, cowl, ramp, Mach number, numerical analysis

## I. INTRODUCTION

A 2D scramjet inlet design for supersonic hydrogen combustion, using shock wave theory and neglecting viscosity. Analysis at Mach 7, 30km shows varying ramp configurations achieve target temperature and Mach number[1]. Hypersonic ramjet engines face 2 limitations: upstream shock waves causing instability and inefficient supersonic combustion. A new "Sod Ramjet" concept replaces combustion with a stable, controllable oblique detonation wave, verified in wind tunnel tests. This approach offers a promising, efficient, and stable solution for hypersonic airbreathing propulsion[2]. Hydrogen-fueled versions show promise for space access and hydrocarbon versions for missiles, collaboration and a focus on healthy flow configurations are crucial. Future exploration of detonation waves and ionised flow manipulation could unlock further potential for truly robust scramjet engines dominating hypersonic flight[3]. A two-dimensional mixed compression scramjet inlet design, optimising for spontaneous hydrogen combustion at Mach 7. The design method considers air as a calorically perfect gas, ensuring consistent shock strength and thermodynamic properties across varying numbers of ramps, making it viable for sustained hypersonic flight[4]. Minimising drag and maximising compression efficiency at two different flight conditions were achieved. Key design factors were identified, and shorter intakes were found to be prone to flow separation. The optimization yielded improved performance with high compression efficiency and moderate drag, suitable for a wide range of flight conditions[5].

Using multiple injection points (better mixing, cooling, and pressure), adjusting injection parameters (impacts fuel penetration and mixing), and modifying the combustor wall (guides fuel and creates mixing shockwaves[6]) Using ANSYS 14-FLUENT, the study reveals that a  $\frac{1}{4}$   $0^\circ$  angle of attack yields the smallest ignition delay and highest efficiency, offering valuable insights into shock structures and combustion phenomena for optimised scramjet performance[7]. Revealing that a slightly lower Mach number than theoretical benefits thrust, while lift increases significantly with Mach number[8]. Utilising computational fluid dynamics (CFD) and CATIA, the analysis identifies a specific ramp angle range ( $4.2^\circ$ ,  $5.2^\circ$ ,  $6.2^\circ$ ) as more suitable, ensuring enhanced fuel-air mixing and achieving desirable thrust[9]. Scramjets ignite fuel by spraying it superfast creating complex interactions with air, shockwaves, and turbulence[10]. Scramjets demand efficient fuel-air mixing for peak performance, a challenge due to fleeting fuel residence time. Researchers explored passive (wall injection, struts) and active (pulsed jets) mixing strategies to enhance this process[11]. Hydrogen emerged as the leader, boasting the highest thrust and efficiency while offering the widest operational speed range. Kerosene, on the other hand, displayed the lowest minimum required speed, showcasing the significant influence fuel selection has on key scramjet performance parameters[12]. Statistical trends suggest a correlation between better basic flow field and improved stream-traced inlet, but exceptions exist [13]. Injection pressure and wedge angle significantly impacted thrust, with combustion playing a key role. Lower injection pressure enhanced mixing and combustion, leading to optimal performance[14]. Struts enhance fuel injection, mixing, and flame stabilisation in scramjet combustors, but require optimization for drag and thermal protection [15]. By rotating ramjets to avoid interference, the combined scramjet-ramjet system functions well at Mach 8 (exceeding drag for sustained flight) despite limitations at lower speed[16] Utilising CFD analysis and optimising the configuration with centrally located scramjet and rotated ramjets. Despite reduced efficiency at other speeds, the system demonstrated effective shock isolation, producing significant thrust for sustained flight[17].

Results from numerical simulations confirm the success of the approach, demonstrating improved total pressure recovery, reduced inviscid drag, and effective flow structure under diverse conditions[18]. Results demonstrated that a morphable waverider inlet significantly improved thrust and specific impulse across a wide range of flight conditions, showcasing enhanced performance over traditional rigid planar inlet designs[19]. Different models for fuel-air mixing and chemical reactions were compared. The most accurate model included information about reaction progress, leading to a better understanding of flame behaviour in supersonic combustion[20]. A moderate cowl contraction ( $b = 4^\circ - 12^\circ$ ) is optimal for isolator starting, while increasing exit blockage leads to pressure rise and influences flow structures, impacting severe separations and shock interactions[21]. Thrust margin and lift-to-drag ratio (L/D) exhibit a trade-off, influenced by shock angles, vehicle volumes, and Mach numbers. Additionally, inlets with minimal height variations show promise for efficient forebody configurations, with altitude limitations imposed by combustor entrance requirement[22].

The introduced modelling and analysis tool-suite bridges the gap between low and high-order models, facilitating multidisciplinary analysis for optimal stability and performance in hypersonic vehicle design[23]. Beyond the record-breaking speeds, these flights yielded valuable data for developing future air breathing hypersonic vehicles. While the NGLT program explored technologies for scramjet-powered space launch[24]. Using a computational design tool, the study indicates comparable performance between scramjet and scramjet configurations, emphasising the importance of refining submodels for improved mixing and combustion efficiency estimates in future research[25]. Combining experiments and simulations confirmed excellent efficiency (85-89%) across most designs. Though needing further refinement to model boundary layer behaviour, this collaborative approach validates tools for future hypersonic inlet design[26]. Subsystem-level design and optimization precede a system-level approach, incorporating multi-fidelity simulation models based on design constraints, with Design of Experiment (DoE) and genetic algorithms (GA) for efficient exploration and solution finding[27] The preliminary analysis of a scramjet combustor pilot reveals promising cold flow mixing efficiency with minimal total pressure losses, supported by favourable preliminary cold flow wall pressure comparisons with experiments[28].

Hypersonic flow refers to the flow of gases at speeds significantly higher than the speed of sound. The term "hypersonic" is generally applied to speeds above Mach 5, where Mach number is the ratio of the flow velocity to the speed of sound in the medium. The speed of sound varies depending on factors such as temperature and composition of the medium. Flow can be classified as subsonic flow: Mach numbers

below 1 (e.g., speeds less than the speed of sound), transonic flow: Mach numbers near 1, supersonic flow: Mach numbers greater than 1 but less than 5, and hypersonic flow: Mach numbers above 5. Hypersonic technology has applications in military and civilian sectors, including rapid-response missile systems, space exploration, and high-speed transportation.

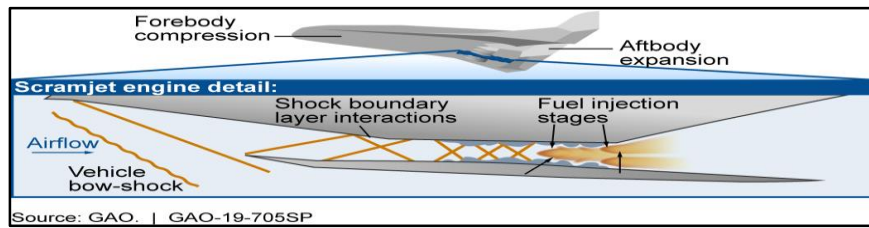
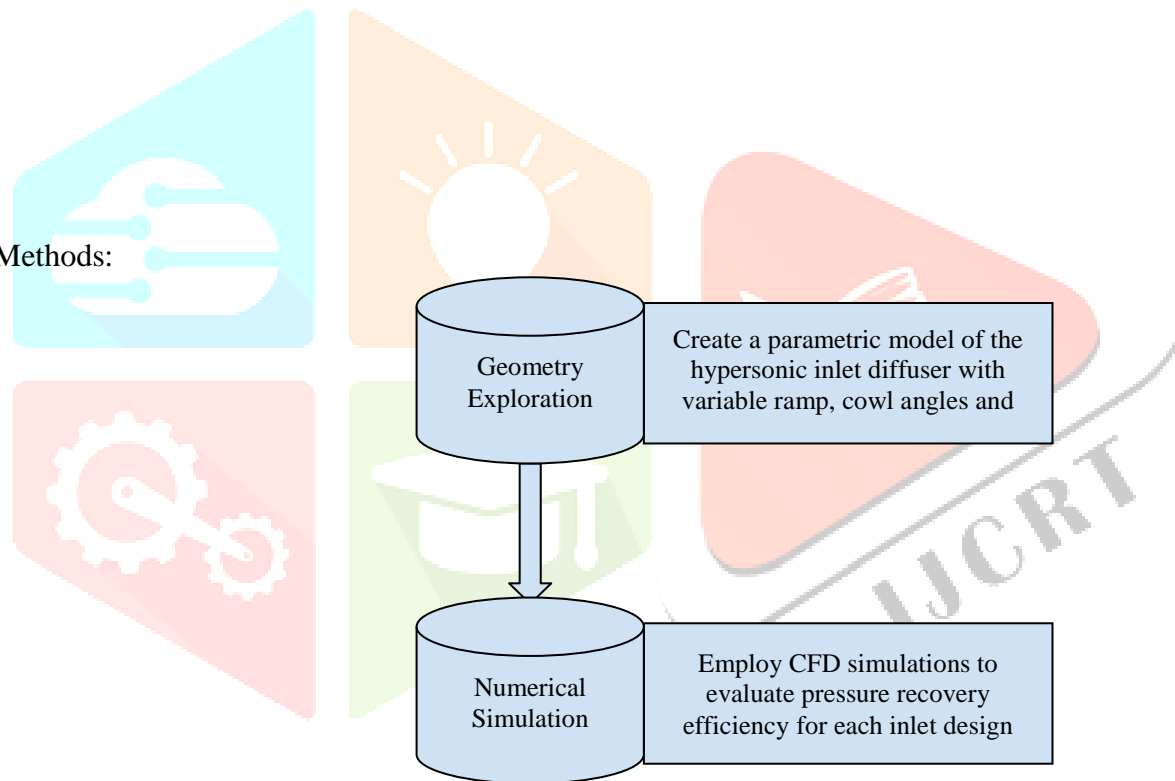


Fig.1:Hypersonic air breathing engine

Traditional hypersonic inlet diffuser faces challenges related to achieving optimal pressure recovery value at suitable Mach numbers at the inlet to the combustor. So, there is a need to have an optimal cowl and ramp design to obtain the highest performance of hypersonic inlet diffuser, further it improves the ramjet engine performance. In this regard an attempt is made to obtain optimal cowl and ramp geometry by numerical analysis.

II Methods:



### III. Numerical Setup:

Hypersonic inlet diffuser was designed in Ansys fluent and obtained 7130 nodes and 6880 elements as shown in the figure 4. Inlet was supplied with pressure of 710 pa at Mach number 10 for all the 32 cases as shown in the table1.

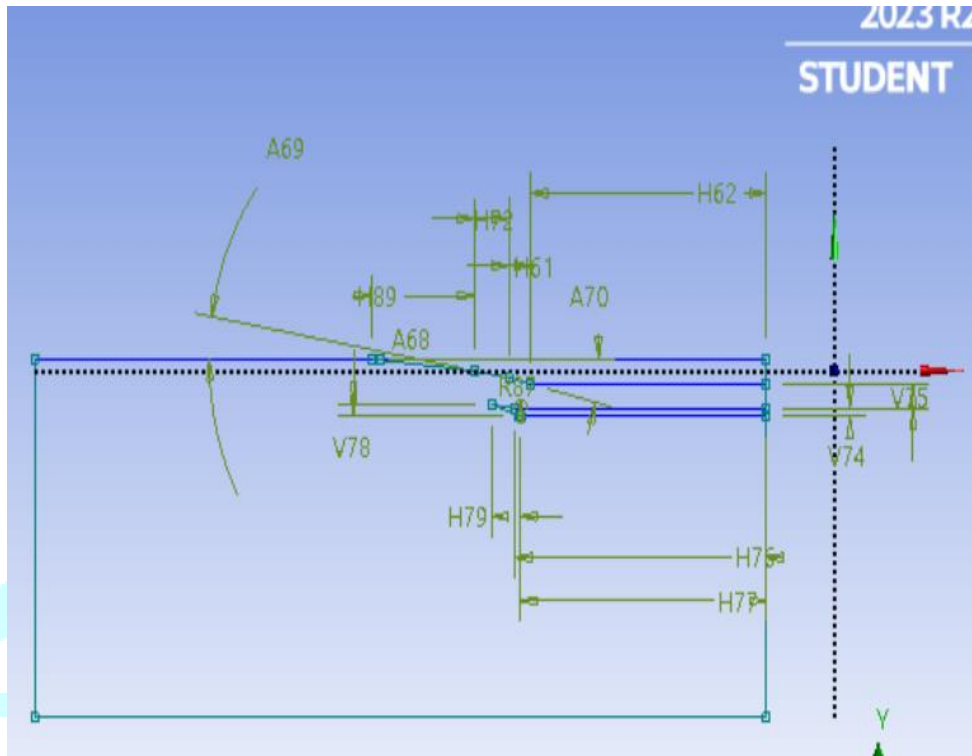


Fig.3: 2-D Sketch and geometry of Supersonic Inlet Diffuser

| Case | Inlet Static Pressure (P <sub>1</sub> ) (Pascals) | Free Stream Mach Number (M <sub>∞</sub> ) | Fist Ramp Angle (θ <sub>1</sub> ) (Degrees) | Second Ramp Angle (θ <sub>2</sub> ) (Degrees) | Third Ramp Angle (θ <sub>3</sub> ) (Degrees) | Fist Ramp Length (L <sub>1</sub> ) (mm) | Second Ramp Length (L <sub>2</sub> ) (mm) | Third Ramp Length (L <sub>3</sub> ) (mm) |
|------|---|---|---|---|--|---|---|--|
| 1    | 710   | 10  | 5   | 8   | 12.35  | 100                                     | 108.46                                    | 70                                       |
| 2    | 710   | 10  | 5   | 11  | 13   | 100                                     | 108.46                                    | 70                                       |
| 3    | 710   | 10  | 5   | 11  | 10   | 100                                     | 108.46                                    | 70                                       |
| 4    | 710   | 10  | 5   | 11  | 12.35  | 400                                     | 108.46                                    | 70                                       |
| 5    | 710   | 10  | 5   | 11  | 12.35  | 450                                     | 108.46                                    | 70                                       |
| 6    | 710   | 10  | 5   | 11  | 12.35  | 500                                     | 108.46                                    | 70                                       |
| 7    | 710   | 10  | 5   | 11  | 12.35  | 550                                     | 108.46                                    | 70                                       |
| 8    | 710   | 10  | 5   | 11  | 12.35  | 600                                     | 108.46                                    | 70                                       |
| 9    | 710   | 10  | 5   | 11  | 12.35  | 650                                     | 108.46                                    | 70                                       |
| 10   | 710   | 10  | 5   | 11  | 12.35  | 700                                     | 108.46                                    | 70                                       |

|    |     |    |   |    |       |     |        |    |
|----|-----|----|---|----|-------|-----|--------|----|
| 11 | 710 | 10 | 5 | 11 | 12.35 | 750 | 108.46 | 70 |
| 12 | 710 | 10 | 5 | 11 | 12.35 | 800 | 108.46 | 70 |
| 13 | 710 | 10 | 5 | 11 | 12.35 | 750 | 120    | 70 |
| 14 | 710 | 10 | 5 | 11 | 12.35 | 750 | 150    | 70 |
| 15 | 710 | 10 | 5 | 11 | 12.35 | 750 | 180    | 70 |
| 16 | 710 | 10 | 5 | 11 | 12.35 | 750 | 200    | 70 |
| 17 | 710 | 10 | 5 | 11 | 12.35 | 750 | 220    | 70 |
| 18 | 710 | 10 | 5 | 11 | 12.35 | 750 | 250    | 70 |
| 19 | 710 | 10 | 5 | 11 | 12.35 | 750 | 300    | 70 |
| 20 | 710 | 10 | 5 | 11 | 12.35 | 750 | 350    | 70 |
| 21 | 710 | 10 | 5 | 11 | 12.35 | 750 | 380    | 70 |
| 22 | 710 | 10 | 5 | 11 | 12.35 | 750 | 400    | 70 |
| 23 | 710 | 10 | 5 | 11 | 12.35 | 750 | 450    | 70 |
| 24 | 710 | 10 | 5 | 11 | 12.35 | 750 | 550    | 70 |
| 25 | 710 | 10 | 5 | 11 | 12.35 | 750 | 700    | 70 |
| 26 | 710 | 10 | 5 | 11 | 12.35 | 750 | 800    | 70 |
| 27 | 710 | 10 | 5 | 11 | 12.35 | 750 | 900    | 70 |
| 28 | 710 | 10 | 5 | 11 | 12.35 | 750 | 950    | 70 |
| 29 | 710 | 10 | 5 | 11 | 12.35 | 750 | 1000   | 70 |
| 30 | 710 | 10 | 5 | 11 | 12.35 | 750 | 900    | 80 |
| 31 | 710 | 10 | 5 | 11 | 12.35 | 750 | 900    | 60 |
| 32 | 710 | 10 | 5 | 11 | 12.35 | 750 | 900    | 70 |

**IV.Results:**

The outlet Mach number and outlet pressure distributions are obtained at constant inlet static pressure of 710 pa and free stream Mach number of 10 for different angle and length of cowl and ramp Numerical analysis was performed for different combination of cowl and ramp angles and length as shown in the table:1.

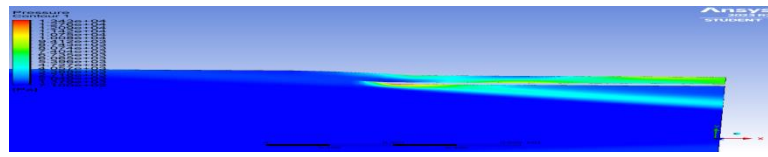


Fig.4: Pressure distribution in hypersonic inlet diffuse for case-1

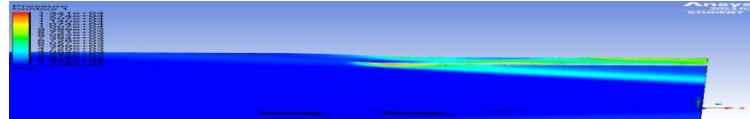


Fig.5:Pressure distribution in supersonic inlet diffuser for case-2

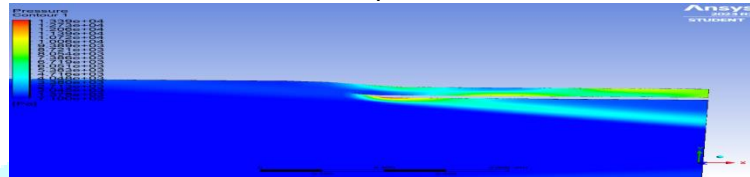


Fig.6: Pressure distribution in supersonic inlet diffuser for case-3

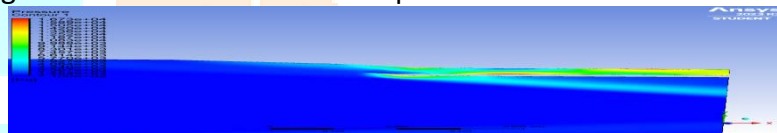


Fig.7: Pressure distribution in supersonic inlet diffuser for case-4

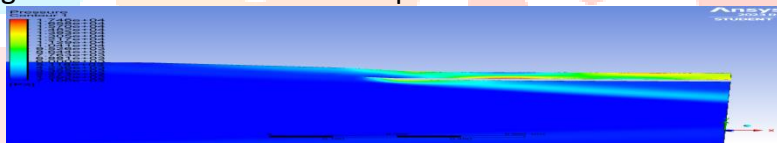


Fig.8: Pressure distribution in supersonic inlet diffuser for case-5

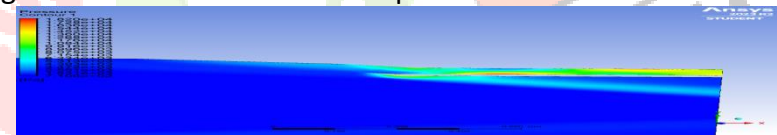


Fig.9: Pressure distribution in supersonic inlet diffuser for case-6

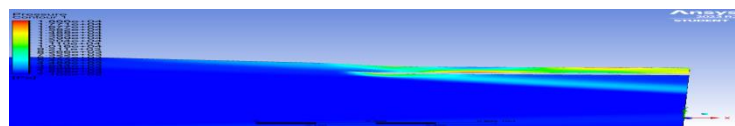


Fig.10:Pressure distribution in supersonic inlet diffuser for case-7

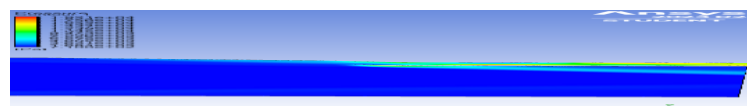


Fig.11:Pressure distribution in supersonic inlet diffuser for case-8

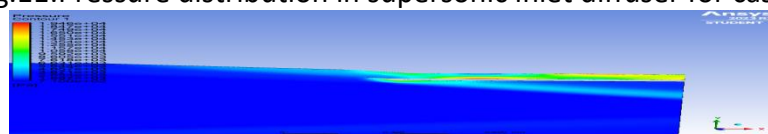


Fig.12:Pressure distribution in supersonic inlet diffuser for case-9



Fig.13:Pressure distribution in supersonic inlet diffuser for case-10

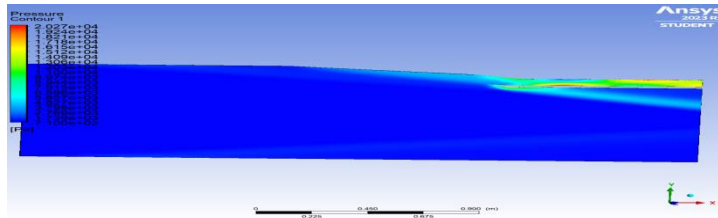


Fig.14:Pressure distribution in supersonic inlet diffuser for case-11

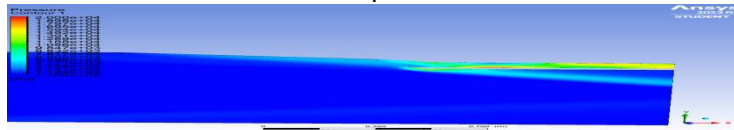


Fig.15:Pressure distribution in supersonic inlet diffuser for case-12

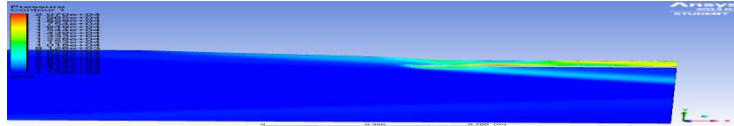


Fig.16 :Pressure distribution in supersonic inlet diffuser for case-13

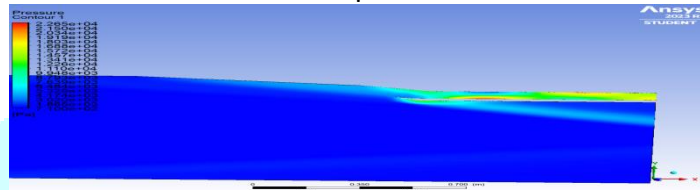


Fig.17: Pressure distribution in supersonic inlet diffuser for case-14

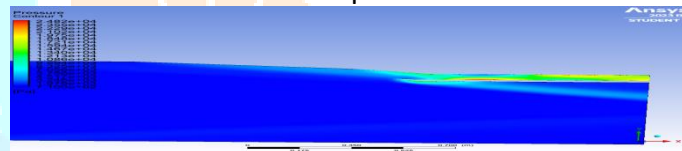


Fig.18:Pressure distribution in supersonic inlet diffuser for case-15

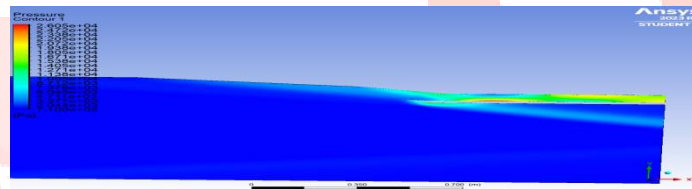


Fig.19:Pressure distribution in supersonic inlet diffuser for case-16



Fig.20:Pressure distribution in supersonic inlet diffuser for case-17

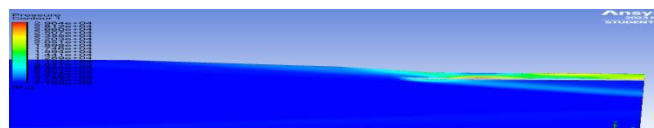


Fig.21:Pressure distribution in supersonic inlet diffuser for case-18



Fig.22:Pressure distribution in supersonic inlet diffuser for case-19



Fig.23:Pressure distribution in supersonic inlet diffuser for case-20

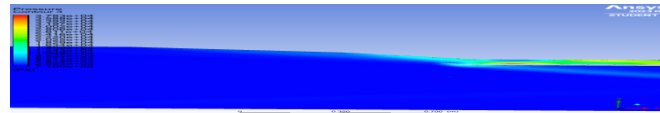


Fig.24:Pressure distribution in supersonic inlet diffuser for case-21

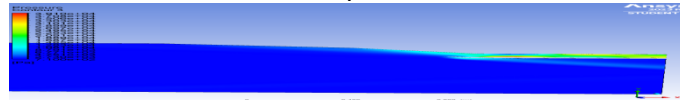


Fig.25:Pressure distribution in supersonic inlet diffuser for case-22

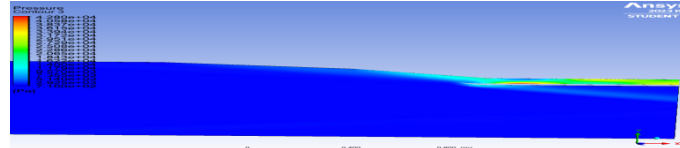


Fig.26:Pressure distribution in supersonic inlet diffuser for case-23

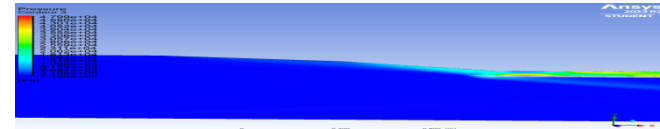


Fig.27:Pressure distribution in supersonic inlet diffuser for case-24

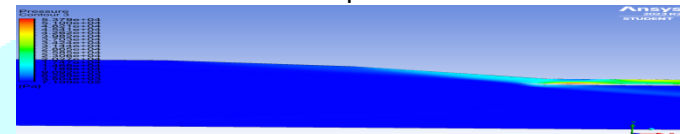


Fig.28:Pressure distribution in supersonic inlet diffuser for case-25

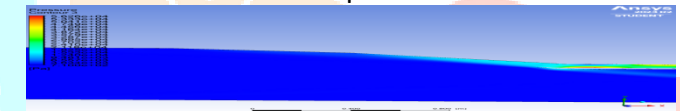


Fig.29: Pressure distribution in supersonic inlet diffuser for case-26

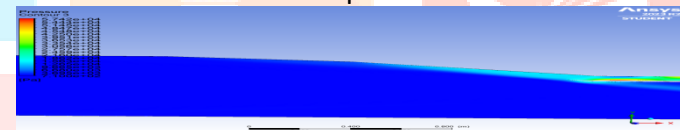


Fig.30:Pressure distribution in supersonic inlet diffuser for case-27

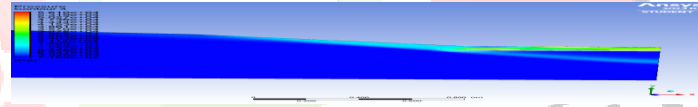


Fig.31:Pressure distribution in supersonic inlet diffuser for case-28

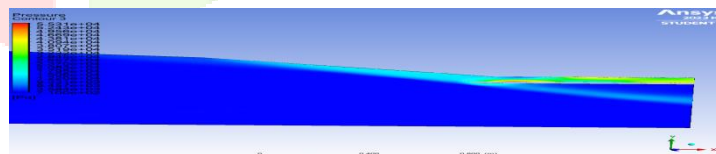


Fig.32: Pressure distribution in supersonic inlet diffuser for case-29

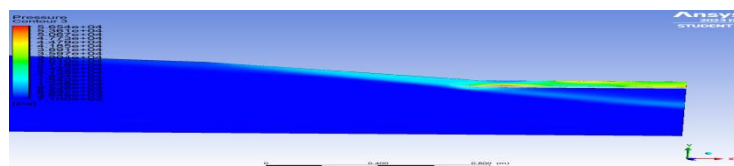


Fig.33:Pressure distribution in supersonic inlet diffuser for case-30

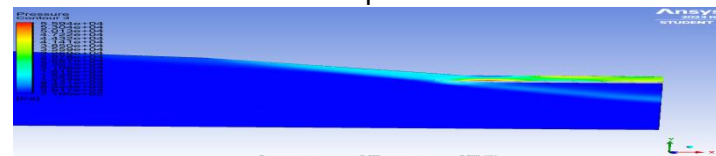


Fig.34:Pressure distribution in supersonic inlet diffuser for case-31



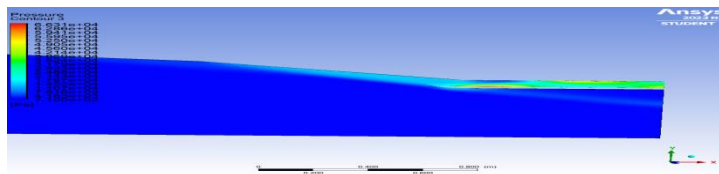


Fig.35:Pressure distribution in supersonic inlet diffuser for case-32

**V.Discussion:**

Outlet pressure, Mach number, temperature, and velocity were plotted for all the 32 cases as shown in the below figures.



Fig.15:Outlet Mach number variation at different cases

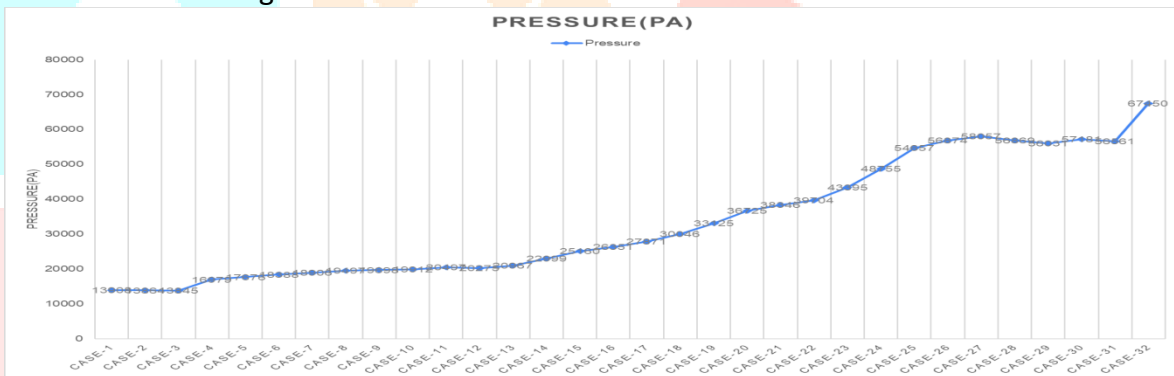


Fig.16: Outlet pressure variation at different cases

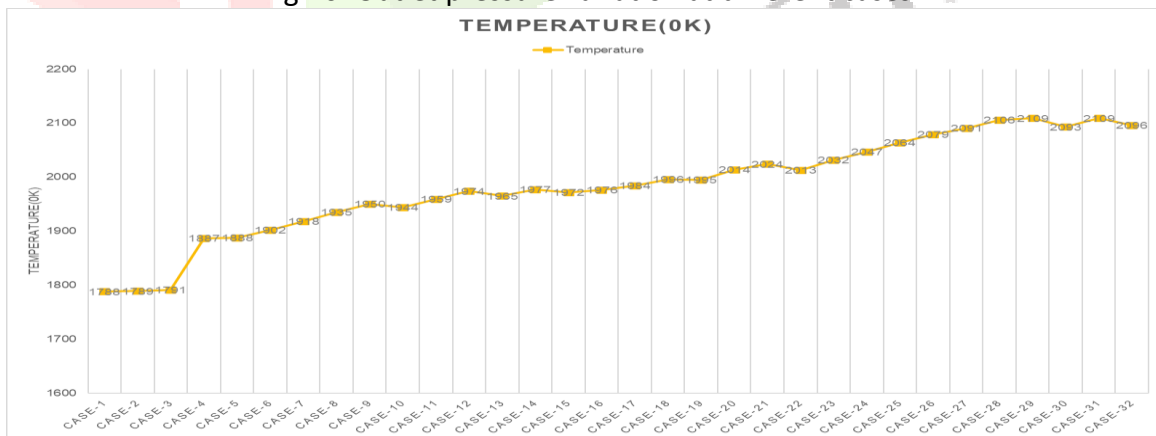


Fig.16:Outlet temperature variation at different cases

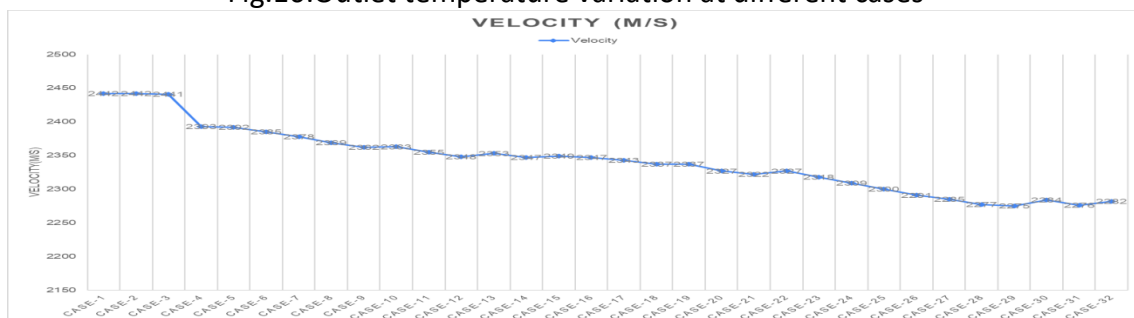


Fig.16: Outlet velocity variation at different cases

Outlet pressure of hypersonic inlet is increased as the cases increases and obtain maximum value i.e 67450 pa at  $\theta_1=5^\circ$ ,  $\theta_2=11^\circ$ ,  $\theta_3=12.35^\circ$ ,  $L_1= 750\text{mm}$ ,  $L_2= 900\text{mm}$ ,  $L_3= 70\text{mm}$ . At these pressures the outlet Mach number lied on 2 to 3, so it was required Mach number for the hypersonic inlet for efficient combustion. And also seen that the pressure distribution is more uniform at that maximum outlet pressure.

## VI. Conclusion:

Performance of hypersonic inlet diffuser affects the performance of ramjet engines. Hypersonic inlet diffuser performance is affected by geometry design of cowl and ramp.hypersonic inlet diffuser was analysed numerically at different cowl and ramp angle and lengths at constant inlet static pressure of 710 pa and free stream Mach number of 10. Total pressure outlet,outletMach number and outlet stagnation pressure were obtained for different cowl and ramp geometries combinations. The optimal Mach number 2.48 and pressure outlet 67450 were obtained at  $\theta_1=5^\circ$ ,  $\theta_2=11^\circ$ ,  $\theta_3=12.35^\circ$ ,  $L_1= 750\text{mm}$ ,  $L_2= 900\text{mm}$ ,  $L_3= 70\text{mm}$  and these conditions more uniform pressure and Mach number were recorded.

## References:

1. Araújo, Pedro PB, et al. "Optimization of scramjet inlet based on temperature and Mach number of supersonic combustion." *Aerospace science and technology* 116 (2021): 106864.
2. Jiang, Zonglin, et al. "Criteria for hypersonic airbreathing propulsion and its experimental verification." *Chinese Journal of Aeronautics* 34.3 (2021): 94-104.
3. Janakiram, S., & Muruganandam, T. M. (2021). Analytically Modeling a Dual-Mode Scramjet with Fuel Flow Rate as the Controlling Parameter. In *Proceedings of the National Aerospace Propulsion Conference* (pp. 449-464). Springer Singapore.
4. Araújo, P. P., Pereira, M. V., Marinho, G. S., Martos, J. F., & Toro, P. G. (2021). Optimization of scramjet inlet based on temperature and Mach number of supersonic combustion. *Aerospace science and technology*, 116, 106864.
5. Brahmachary, Shuvayan, Chihiro Fujio, and Hideaki Ogawa. "Multi-point design optimization of a high-performance intake for scramjet-powered ascent flight." *Aerospace Science and Technology* 107 (2020): 106362.
6. Choubey, G., Yuvarajan, D., Huang, W., Shafee, A., & Pandey, K. M. (2020). Recent research progress on transverse injection technique for scramjet applications-a brief review. *International Journal of Hydrogen Energy*, 45(51), 27806-27827.
7. Paramasivam, K., Dhas, A. A. G., Joy, N., Balakrishnan, K., Harsha, V. S., & Yuvaraj, R. (2020, December). Design and analysis of an inlet and combustion chamber of scramjet engine. In *AIP Conference Proceedings* (Vol. 2311, No. 1). AIP Publishing.
8. Yu, K., Chen, Y., Huang, S., Lv, Z., & Xu, J. (2020). Optimization and analysis of inverse design method of maximum thrust scramjet nozzles. *Aerospace Science and Technology*, 105, 105948.
9. Paramasivam, K., Dhas, A. A. G., Joy, N., Balakrishnan, K., Harsha, V. S., & Yuvaraj, R. (2020, December). Design and analysis of an inlet and combustion chamber of scramjet engine. In *AIP Conference Proceedings* (Vol. 2311, No. 1). AIP Publishing.
10. Ren, Z., Wang, B., Xiang, G., Zhao, D., & Zheng, L. (2019). Supersonic spray combustion subject to scramjets: Progress and challenges. *Progress in Aerospace Sciences*, 105, 40-59.
11. Huang, W., Du, Z. B., Yan, L., & Xia, Z. X. (2019). Supersonic mixing in airbreathing propulsion systems for hypersonic flights. *Progress in Aerospace Sciences*, 109, 100545.
12. Zhi-hua, W., Yu-chun, C., Xiao-dong, W., Min-ze, C., Jun-hui, Z., & Chi, L. (2019, July). Influence of different fuels on scramjet engine performance. In *2019 IEEE 10th International Conference on Mechanical and Aerospace Engineering (ICMAE)* (pp. 434-438). IEEE.
13. Xiong, B., Fan, X. Q., & Wang, Y. (2019). Parameterization and optimization design of a hypersonic inward turning inlet. *Acta Astronautica*, 164, 130-141.
14. Candon, M. J., and Hideaki Ogawa. "Numerical analysis and design optimization of supersonic after-burning with strut fuel injectors for scramjet engines." *Acta Astronautica* 147 (2018): 281-296.

15. Chang, Juntao, et al. "Research progress on strut-equipped supersonic combustors for scramjet application." *Progress in Aerospace Sciences* 103 (2018): 1-30.
16. sen, D., Pesyridis, A., & Lenton, A. (2018). A scramjet compression system for hypersonic air transportation vehicle combined cycle engines. *Energies*, 11(6), 1568.
17. Wang, J., Cai, J., Duan, Y., & Tian, Y. (2017). Design of shape morphing hypersonic inward-turning inlet using multistage optimization. *Aerospace Science and Technology*, 66, 44-58.
18. Goodwin, G. B., & Maxwell, J. R. (2017). Performance analysis of a hypersonic scramjet engine with a morphable waverider inlet. In *53rd AIAA/SAE/ASEE Joint Propulsion Conference* (p. 4651).
19. Choubey, G., & Pandey, K. M. (2016). Effect of variation of angle of attack on the performance of two-strut scramjet combustor. *international journal of hydrogen energy*, 41(26), 11455-11470.
20. Zhi, C., Yi, S., Zhu, Y., Wu, Y., Zhang, Q., & Quan, P. (2014). Investigation on flows in a supersonic isolator with an adjustable cowl convergence angle. *Experimental thermal and fluid science*, 52, 182-190.
21. Roberts, Kristen, and Donald Wilson. "Analysis and design of a hypersonic scramjet engine with a transition Mach number of 4.00." *47th AIAA aerospace sciences meeting including the new horizons forum and aerospace exposition*. 2009.
22. Kelkar, A., Vogel, J., Inger, G., Whitmer, C., Sidlinger, A., & Ford, C. (2009, October). Modeling and analysis framework for early stage trade-off studies for scramjet-powered hypersonic vehicles. In *16th AIAA/DLR/DGLR International Space Planes and Hypersonic Systems and Technologies Conference* (p. 7325).
23. Voland, R. T., Huebner, L. D., & McClinton, C. R. (2006). X-43A hypersonic vehicle technology development. *Acta Astronautica*, 59(1-5), 181-191.
24. Xu, X., Dajun, X., & Guobiao, C. (2005). Optimization design for scramjet and analysis of its operation performance. *Acta Astronautica*, 57(2-8), 390-403.
25. Reinartz, B. U., Herrmann, C. D., Ballmann, J., & Koschel, W. W. (2003). Aerodynamic performance analysis of a hypersonic inlet isolator using computation and experiment. *Journal of Propulsion and Power*, 19(5), 868-875.
26. Curran, E. T. (2001). Scramjet engines: the first forty years. *Journal of Propulsion and Power*, 17(6), 1138-1144.
27. Molvik, G., Bowles, J., & Huynh, L. (1993). A hypersonic waverider research vehicle with hydrocarbon scramjet propulsion-Design and analysis. In *5th International Aerospace Planes and Hypersonics Technologies Conference* (p. 5097).
28. O'Neill, M. K. L., & Lewis, M. J. (1992). Optimized scramjet integration on a waverider. *Journal of Aircraft*, 29(6), 1114-1121.